THE ASTROPHYSICAL JOURNAL, 253:949–962, 1982 February 15

THE ENERGY SPECTRUM OF 20 keV–20 MeV ELECTRONS ACCELERATED IN LARGE SOLAR FLARES

R. P. LIN
Space Sciences Laboratory, University of California-Berkeley
R. A. MEWALDT
California Institute of Technology
M. A. I. VAN HOLLEBEKE
Goddard Space Flight Center
Received 1981 May 5; accepted 1981 August 24

ABSTRACT

We present *IMP 6*, *7*, and *8* measurements of the energy spectrum of 20 keV to 20 MeV electrons observed from large solar flares. To minimize propagation effects, only events from flares located at W30° to W90° solar longitude were chosen for study. The energy spectra were constructed using the maximum flux observed at each energy. These spectra are shown to be representative of the spectra of the electrons escaping from the Sun over this range of energies. We find that every event shows the same spectral shape: a double power law with a smooth transition around 100–200 keV and power law exponents of 0.6–2.0 below and 2.4–4.3 above. The more intense the event, the harder the spectrum observed. In some cases the spectra are observed to steepen above 3 MeV. The spectra are generally similar to those inferred from hard X-ray and microwave measurements, and the peak >20 keV electron flux is well correlated with the peak microwave emission at 10 cm. These findings indicate that the observed electron spectra are representative of the accelerated electron spectra at the Sun. Thus, a double power law appears to be the characteristic spectral shape produced in flare second phase acceleration. Comparisons with proton spectra from the same events suggest that the acceleration is velocity dependent. The shock waves observed in these large flare events are likely to be the accelerating agent.

Subject headings: particle acceleration — Sun: flares — Sun: X-rays

I. INTRODUCTION

Large solar flares are the most energetic natural particle accelerators found in the solar system, occasionally accelerating ions to tens of GeV and electrons to hundreds of MeV energies. The accelerated particles can be studied indirectly, via observations of the electromagnetic emissions produced by the particles in their interactions with the solar atmosphere, or directly by spacecraft and ground-based observations of the particles which escape into the interplanetary medium. The electromagnetic emissions (X-ray, gamma ray, and radio emission) depend critically on ambient conditions in the solar atmosphere where the accelerated particles reside (the density, magnetic field, and temperature), while the interpretation of the particle fluxes observed in the interplanetary medium depend on the characteristics of the escape and interplanetary propagation processes.

Radio, X-ray and gamma ray, and energetic particle observations indicate that there are two distinct acceleration processes associated with solar flares (Wild, Smerd, and Weiss 1963; Frost and Dennis 1971; Lin 1971, 1974; Lin and Hudson 1976; Bai and Ramaty 1977). During the impulsive or flash phase electrons are often accelerated to ~10–100 keV energies, even in small flares or subflares. For some flares, the energy contained in these electrons may be a substantial fraction of the total flare energy. Thus the primary energy release mechanism for flares may initially convert stored magnetic energy into energetic electrons. These electrons can produce most of the observed impulsive phase flare phenomena through their interactions with the solar atmosphere. In large flares a second acceleration sometimes occurs which accelerates both ions and electrons to MeV energies and above. This second acceleration appears to have a close association with shock waves in the solar atmosphere as observed by type II radio bursts.

Other acceleration processes distinct from these two may exist. For example, the spectral shape of the gamma ray continuum for the 1972 August 4 large flare suggests that the electron spectrum above ~100 keV may consist of two components, a power law up to ~1 MeV and an additional flatter component above ~1 MeV (Ramaty *et al.* 1975), although another interpretation of the

flattening in terms of nuclear gamma ray continuum (Ramaty, Kozlovsky, and Suri 1977) is possible. Also the 10–100 keV electrons responsible for type III radio bursts, which are commonly observed even in the absence of flares, may be accelerated by a separate mechanism. Recently, impulsive electron events observed only at energies below ~10 keV were discovered (Potter, Lin, and Anderson 1980). These events appear to be the most common type of impulsive acceleration by the Sun observed directly in the interplanetary medium, but they are not associated with reported chromospheric flares.

We here present the results of a study of the electron spectrum observed directly by spacecraft in the near Earth interplanetary medium following large solar flares. This study provides the first compilation of flare electron spectra over a wide energy range, from ~20 keV to ≥20 MeV, with good energy resolution (see Lin 1974 and Simnett 1974 for reviews of previous work). The aim of this study was to obtain information on the spectrum of the accelerated electrons at the Sun. The effects of interplanetary propagation were minimized wherever possible. We show that over this energy range the spectrum constructed from the maximum flux at each energy observed at 1 AU is representative of the spectrum of electrons escaping from the Sun. We find that these spectra have a characteristic double power law shape for large flare events. This finding provides significant constraints on the mechanisms of particle acceleration and the generation of radio, X-ray, and gamma-ray emissions in solar flares.

II. EXPERIMENTAL DETAILS

The observations were made with three different instruments: the University of California, Berkeley (UCB), energetic particle experiment on the *IMP 6* spacecraft; the Caltech cosmic ray experiment on *IMP 7* and *IMP 8*; and the Goddard Space Flight Center (GSFC) cosmic ray experiment on *IMP 7* and *IMP 8*. The instruments used here have been carefully cross-calibrated in the regions of energy overlap to insure accurate relative energy spectra.

The UCB instrument consists of two passively cooled semiconductor detector telescopes and two Geiger-Müller detectors. A detailed description is contained in Lin, Meng, and Anderson (1974). All the observations used here come from one telescope, P3, which opens directly into space, has no foil covering, and consists of three solid state detectors: the first measures the energy of stopping particles, the second element forms a telescope with the first, and the third provides anticoincidence against penetrating particles. The telescope is pointed to within 10° of the spin axis, itself aligned normal to the ecliptic plane, and is carefully collimated to eliminate scattered sunlight. This telescope measures both electrons from 18 to ~300 keV and protons from ~29 keV to 2 MeV. In almost all of the events analyzed here the energetic electrons rise and reach maximum flux before any protons below 300 keV arrive, so that uncontaminated electron spectra can be obtained. In order to take advantage of the high inherent energy resolution of the cooled surface barrier detectors in the P3 assembly, the output is pulse height analyzed into 64 channels through the spacecraft on-board computer. Each channel is about 8 keV wide. This is approximately the full width at half-maximum energy resolution of the detectors for electrons and protons.

On 1971 March 13, *IMP 6* was launched into an eccentric equatorial orbit with an apogee of 211,251 km. This spacecraft spends most of its time outside the Earth's magnetosphere and bow shock but also passes through all regions of terrestrial trapped radiation from the distant radiation zones to the inner radiation belts. Data were obtained essentially continuously until the spacecraft reentered the Earth's atmosphere in 1974 October.

Electrons in the energy interval from 0.16 to ~3 MeV are measured by the Caltech Electron/Isotope Spectrometers on *IMP 7* (Hurford *et al.* 1974) and *IMP 8* (Baker and Stone 1977). Each instrument consists of a stack of 11 silicon solid-state detectors surrounded by a plastic scintillator anticoincidence cup. This study makes use of the "narrow geometry" analysis mode (Hurford *et al.* 1974) in which incident particles are actively collimated to pass through a 50 μm thick detector, D2. Electrons and nuclei are unambiguously identified by a combination of their energy loss in D2, and their total energy loss and range in the remainder of the detector stack. As discussed in Mewaldt, Stone, and Vogt (1978), a background of electron-like events with essentially constant rate results from secondary electrons produced by the interaction of γ rays within the telescope. This background, which is monitored by a separate instrument analysis mode, has been subtracted from the observed pulse height distributions before they are unfolded to produce energy spectra. In the 0.2 to 1 MeV interval, the magnitude of the background subtraction was typically <5% of the observed counting rate and amounted to ~30% in the worst case.

Both Caltech instruments have undergone extensive laboratory calibration with monoenergetic electron beams from a beta spectrometer. Data were taken at 20 energies from 0.1 to 3.3 MeV and at 10 different incidence angles, from which response matrices appropriate to an isotropic flux were derived. The typical energy resolution for a monoenergetic beam (limited by the channel width of the pulse height analyzers) is ~15% FWHM. Although somewhat energy dependent, the nominal geometry factors are 0.07 cm^2 sr for *IMP 7* and 0.23 cm^2 sr for *IMP 8*. Energy spectra from the two instruments are in excellent agreement (see, e.g., Fig. 6). The spectra presented are spin-averaged over directions within ~20° of the ecliptic plane.

The University of California and Caltech experiments overlap in energy coverage between 160 and 342 keV.

Although the detectors in the two experiments point in different directions, it was found through comparisons of the solar electron events that the electron flux levels in the overlap region consistently agreed, provided a constant normalization factor of 0.7 was applied to the University of California data. This factor is within the errors of determining the geometric factors for the two experiments.

The Goddard Medium Energy Dectector (MED) on *IMP 7* and *IMP 8* is used for the >4 MeV electron measurements. This system is a modified version of the *IMP 4* MED, whose operation and calibration has previously been described in detail (Simnett and McDonald 1969). The significant change for electron studies was to extend the cylindrical anticoincidence counter to shield the side areas of the detector completely. The front element is a thin (0.45 g cm^{-2}) CsI crystal (D), which serves as a dE/dx detector. It is operated in coincidence with a thick (9 g cm^{-2}) CsI element (E), which serves as the E detector in a dE/dx-E telescope. As mentioned previously, the sides of the detector are protected by a plastic scintillator anticoincidence guard counter (G), and a fourth element, a thin CsI counter (F) mounted on the base of the E counter, completes the anticoincidence cup. Stopping particles are defined by the logic requirement $DE\bar{F}\bar{G}$. In analyzing the data, a matrix of dE/dx versus E is generated for stopping particles. Electrons produce a pulse in dE/dx similar to that of singly charged minimum-ionizing particles. The distributions, however, become sharper with increasing energy due to the smaller effects of scattering. This "electron line" lies well below that produced by stopping protons. The primary source of background in the electron region is from secondary γ-rays which Compton scatter in the E detector. These γ-rays are generated by high energy nuclear interactions in the spacecraft. This effect is small for galactic cosmic ray measurement and is even less important for solar cosmic rays studies where the average particle energy is much less. Between 4 and 8 MeV, the efficiency for the detection of electrons is 92% and drops to 80% at 12 MeV.

The Goddard and Caltech electron measurements have been intercompared for eight large solar events observed between 1973 and 1977. The intensities at 3 MeV deduced from the two experiments are closely correlated over a flux range of a factor of 45. The Goddard absolute intensity, however, was found to be on average a factor of 2.2 ± 0.5 below that obtained from the Caltech experiment. This should be taken as an indication of the possible systematic uncertainty in intercalibration of the instruments at ~3 MeV. We have not corrected for this apparent difference. Because the Goddard experiment views ~60° out of the ecliptic plane, it is possible that anisotropies in the electron flux may contribute to this difference.

IMP 7 was launched in 1972 September into an approximately circular orbit of ~34 R_E, while the orbital radius of *IMP 8* (launched in 1973 October) ranges from ~24 to ~45 R_E. Both satellites therefore spend a majority of their time in interplanetary space outside the Earth's magnetosphere. In three cases the *IMP 7/8* spectra were obtained inside the Earth's magnetotail (1972 December 16, 1973 September 7, and the *IMP 8* spectrum from 1973 November 3). Note, however, that the *IMP 8* spectrum (inside the magnetotail) is in excellent agreement with that from *IMP 7* (outside the magnetotail) for the 1973 October 3 event. In no case was significant contamination by magnetospheric electrons observed. Essentially continuous data were obtained from the Caltech and Goddard instruments on *IMP 7* until the end of the mission in 1978. Both instruments on *IMP 8* were still in operation as of 1981 April.

III. ANALYSIS METHOD

The electron events for study were chosen in the following manner. All impulsive solar electron events which had statistically significant electron fluxes above ~200 keV and which were observed by *IMP 6* and either *IMP 7* or *IMP 8* were considered. For each event the associated solar flare was identified where possible. To minimize propagation effects only events from flares located between W30° and W90° longitude were selected for study. Events which were contaminated by terrestrial particle fluxes near the time of maximum solar particle flux were eliminated. Table 1 lists all the remaining events observed in the approximately two-year period, along with the associated flare and solar radio phenomena. Note that these nine events had remarkably similar characteristics: almost all were accompanied by type II, III, and IV radio emission, and all had energetic protons as well. These characteristics are typical of large proton flare events as opposed to the small "pure" 10–100 keV electron events (Lin 1971, 1974).

For each event the energy spectrum was constructed by taking the maximum flux in each energy interval. As will be shown, the maximum flux is relatively insensitive to the details of the propagation in the interplanetary medium. The times of maximum flux generally differ for different energies due to velocity dispersion. For these W30° to 90° solar longitude flare events the time to maximum is usually less than a few hours, far shorter than the travel time for the solar wind from the Sun to 1 AU. Thus the propagation of the electrons is effectively that of a fast particle through a stationary magnetic field pattern. Energy changes due to convective effects are therefore likely to be negligible up through the time of maximum flux. (Energy changes due to fast particle-plasma interactions, however, can not be ruled out at present.)

The electron propagation through the interplanetary medium can therefore be treated by the standard diffusion treatment without considering energy changes. Following Parker (1963) and Krimigis (1965) we assume

TABLE 1

SELECT SOLAR FLARE ELECTRON EVENTS, 1972 OCTOBER–1974 SEPTEMBER[a]

DATE	ONSET UT	MAXIMUM UT	PEAK ~ 10^2 keV ELECTRON FLUX (cm^2 sec·sr·keV)$^{-1}$	ENERGETIC PROTONS	ASSOCIATED FLARE							PEAK 10 cm. MICROWAVE BURST s.f.u.	SPECTRAL RADIO EMISSION	SPECTRUM PARAMETERS		
					IMPORTANCE	START	MAX	END	LOCATION		McMATH PLAGE #			BREAK ENERGY (keV)	POWER LAW INDEX < 100 keV	POWER LAW INDEX > 200 keV
1972																
25 Nov	0900	0930–1015	4.7	Yes	1B	0820	0830	0911	S06	W44	12155	238	II, III, IV	105	1.3±0.1	4.3±0.1
28 Nov	0440	0545–0730	0.6	Yes	1N	0355	0403	0426	S08	W80	12115	25	II, III, IV, V	180	1.85±0.1	3.7±0.2
16 Dec	(0400)	0600–0800	2.5	Yes	1B	0344	0349	0440	N12	W57	12136	410	II, III, IV, V	175	1.7±0.2	4.3±0.2
1973																
29–30 Apr	2150	0000–0250 (30th)	12	Yes	2B	2056	2104	2238	N14	W73	12322	2551	II, III, IV	150	0.6±0.1	2.4±0.1
7 Sep	1225	1300–1445	15	Yes	2B	1141	1212	1342	S18	W46	12507	381	II, III, IV	130	1.1±0.1	2.8±0.1
3 Nov[b]	>0105 <0130	0215–0500	3	Yes	2N	0012	0034	0101	S18	W85	12584	227	II, III, IV, V	140	1.3±0.1	3.6±0.1
1974																
15 Jan	>1135 <1235	1300–1345	0.15	Yes	2N	1050	1056	1124	N07	W88	12686	41	No coverage	140	2.0±0.1	3.7±0.2
20 Feb	1545	1630–1700	1.3	Yes	-B	1514	1516	1533	S18	W31	12752	30	III, IV, V	135	2.0±0.2	3.9±0.1
13 May[c]	2130	2130–2200	2.5	Yes	2N	2118	2128	2328	S13	W66	12915	203	II, III, V	80	1.4±0.1	4.3±0.3

a See text for selection criteria

b Some terrestrial proton contamination below 100 keV

c Scatter-free event

(1) that particles diffuse in a random walk through a medium of static scattering centers, (2) that the scattering is isotropic, and (3) that particles neither gain nor lose energy in the scattering process; but that (4) the density of scattering centers varies with radial distance r from the Sun. To obtain an explicit solution we assume a specific form for the spatial dependence of the diffusion coefficient D, namely

$$D = Mr^{\beta},$$

where β and M are parameters independent of r but possibly dependent on particle energy. Then the diffusion equation for isotropic scattering of particles of a given energy is

$$\frac{\partial \rho}{\partial t} = \frac{1}{r^{\alpha}} \frac{\partial}{\partial r}\left(Mr^{\alpha+\beta} \frac{\partial \rho}{\partial r} \right). \tag{1}$$

Here ρ is the number of particles per unit volume at position r, at time t, of energy E; and α is the parameter specifying the dimensionality of the space to be used. The solution to this is

$$\rho(r,t) = \frac{NC(\alpha,\beta)}{(Mt)^{(\alpha+1)/(2-\beta)}} \exp\left[-\frac{r^{2-\beta}}{Mt(2-\beta)^2} \right], \tag{2}$$

where N is the total number of particles released and

$$C(\alpha,\beta) = \frac{(2-\beta)^{-(2\alpha+\beta)/(2-\beta)}}{\Gamma[(\alpha+1)/(2-\beta)]} \tag{3}$$

is a function only of α and β. The time of maximum, t_m, is obtained by setting $\partial\rho/\partial t = 0$.

$$t_m = \frac{r^{2-\beta}}{M(2-\beta)(\alpha+1)} \tag{4}$$

and the maximum density is given by

$$\rho_m = NC(\alpha,\beta)\left[\frac{r^{2-\beta}}{(2-\beta)(\alpha+1)} \right]^{-(\alpha+1)/(2-\beta)} \times \exp\left(-\frac{\alpha+1}{2-\beta} \right). \tag{5}$$

Note that ρ_m does not depend on M at all. The implication of this is that as long as the spatial dependence of the diffusion coefficient (given by β) is the same for different energy particles, the energy spectrum constructed using the maximum flux at each energy reflects the injection spectrum at the Sun, regardless of the variation of the diffusion coefficient (M) with energy. By studying the time profile at different energies, some information on the variation of β with energy can be obtained. Taking the logarithm of both sides of equation (2) we obtain:

$$\log\left[\rho t^{(\alpha+1)/(2-\beta)} \right] = -\left[\frac{r^{2-\beta}}{M(2-\beta)} \right] \frac{1}{t} + \text{constant}. \tag{6}$$

Thus the plot of $\log[\rho t^{(\alpha+1)/(2-\beta)}]$ versus $1/t$ should yield a straight line for the correct value of β.

This analysis was performed on the 1973 September 7 solar particle event shown in Figure 1. Figure 2 shows that a $(\alpha+1)/(2-\beta)$ value of 1.5 ± 0.25 is consistent with the electron propagation for all electron energies from ~20 keV to above ~10 MeV. This result implies that the spectrum constructed with the maximum flux for each energy interval observed at 1 AU is representative of the spectrum of electrons released at the Sun. For three-dimensional propagation (similar results are obtained for one-dimension) $\alpha = 2$ and therefore $\beta = 0$, a value consistent with a recent *Pioneer 10* and *Pioneer 11*

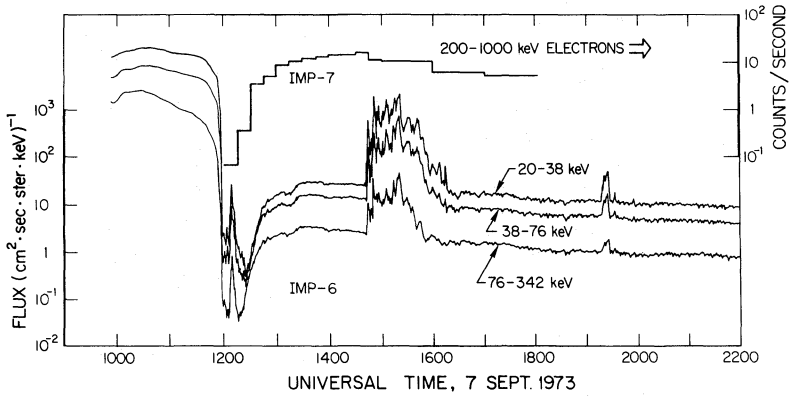

FIG. 1.—The 1973 September 7 solar electron event. The Earth's magnetospheric trapped radiation is observed by *IMP 6* prior to 1200 UT, and some upstream and magnetosheath particles are observed at ~1210 UT and ~1440–1600 UT. The Caltech 200–1000 keV electron profile from *IMP 7* is shown on top.

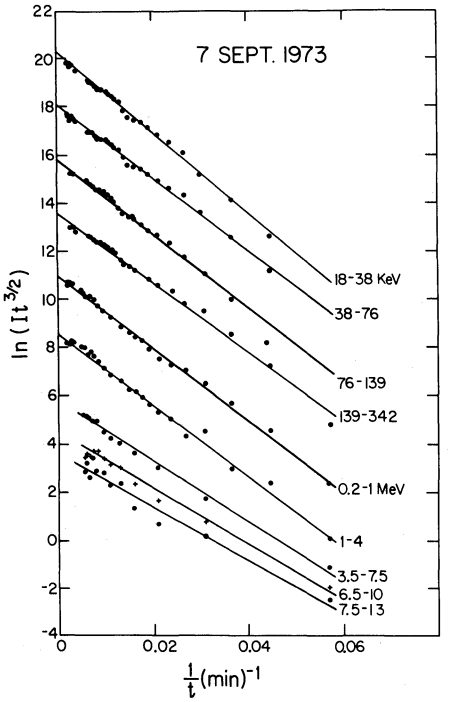

FIG. 2.—An analysis of the 1973 September 7 electron event showing that for all energies from ~20 keV to ~10 MeV the flux varies as $t^{-3/2}\exp(-A/t)$ where A is a constant. The fact that a single power law exponent of 3/2 fits all the energies implies that the radial variation of the diffusion coefficient is the same for all energies (see text).

study (Hamilton 1977; see also references therein). The number of electrons escaping from the Sun is then

$$\frac{dN}{dE} = 4.5\times 10^{40}\left(\frac{1}{v}\right)\frac{dJ}{dE}, \qquad (7)$$

where v is the electron velocity. The analysis also gives a diffusion coefficient, M, at 1 AU, that is roughly constant over this energy range (20 keV to ~10 MeV), with values of ~ 6–8×10^{21} cm^2 s^{-1}, typical of values for diffusive profile electron events (see Lin 1974). Only a few of the other events studied here could be similarly analyzed because observations over an extended time period are required, but a single value of β appears consistent over this energy range for other events as well. One of the observed electron events (1974 May 13) appears to be scatter free, that is, the time profiles suggest means free paths of order ~0.1 AU. Numerical solutions to the telegraph equation, however, indicate that up to mean free paths of ~0.3 AU the above relationship between N and ρ_{max} still holds (Lin, Wang, and Fisk, unpublished work; also Lin 1974).

We have therefore assumed in the following analysis that the injection spectrum is given by the spectrum taken at maximum at each energy. For each event an interval of from a few minutes to ~2 hours at time of maximum was used to obtain a statistically significant maximum rate. The pre-event background was then subtracted to obtain the injection spectrum.

IV. RESULTS

Figure 3 shows the electron energy spectrum for the 1973 September 7 event obtained in the above manner. For this event no pulse height information is available from the *IMP 6* onboard computer. The bars indicate the UCB rate channels which extend up to 340 keV. At energies above 160 keV the measurements of the Caltech instrument are indicated by the solid dots. Note the agreement between the UCB and Caltech measurements in the region of overlap. At energies above ~3 MeV the measurements of the GSFC experiment show that the electron spectrum extends to ≥20 MeV and may steepen above ~2 MeV.

Figure 4 shows the event of 1972 November 25. Terrestrial particle fluxes at energies ≲100 keV are present from ~1030 onward but are not significant at

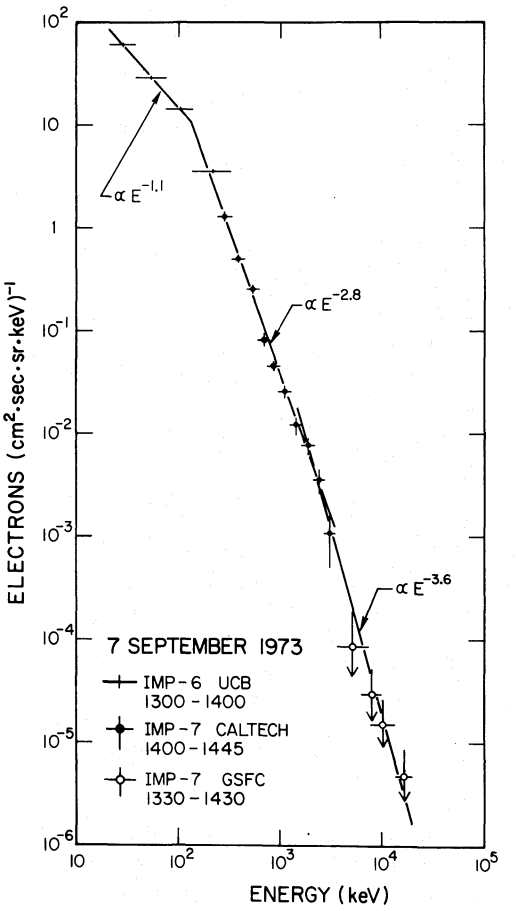

FIG. 3.—The spectrum of the 1973 September 7 event constructed from the maxima observed at each energy.

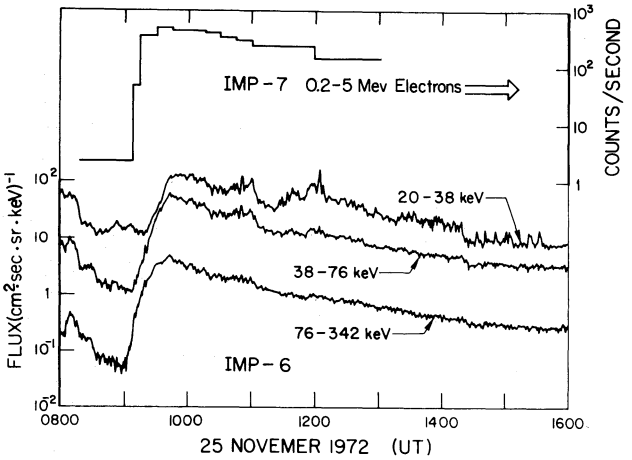

FIG. 4.—The 1977 November 25 solar electron event. Upstream terrestrial particles are present at *IMP 6* prior to the event onset at ~0900 and also sporadically between ~1030 and 1530 UT.

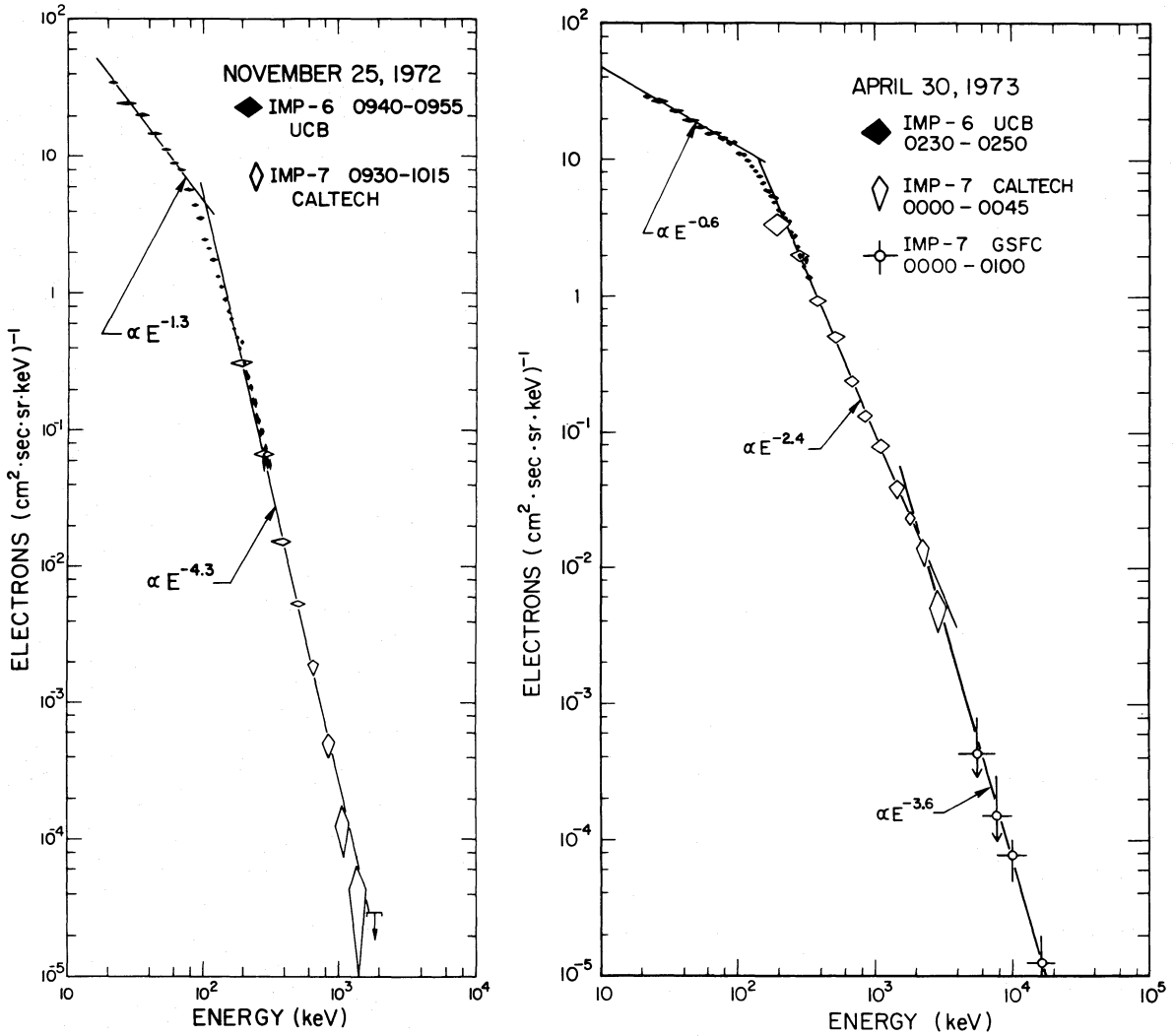

FIG. 5.—The energy spectra for the 1972 November 25 and 1973 April 30 events. For both these events, pulse height analyzer data are available on *IMP 6* to provide very high energy resolution. Both events show a smooth transition between ~100 and 200 keV. Some steepening is observed above ~3 MeV for the April event.

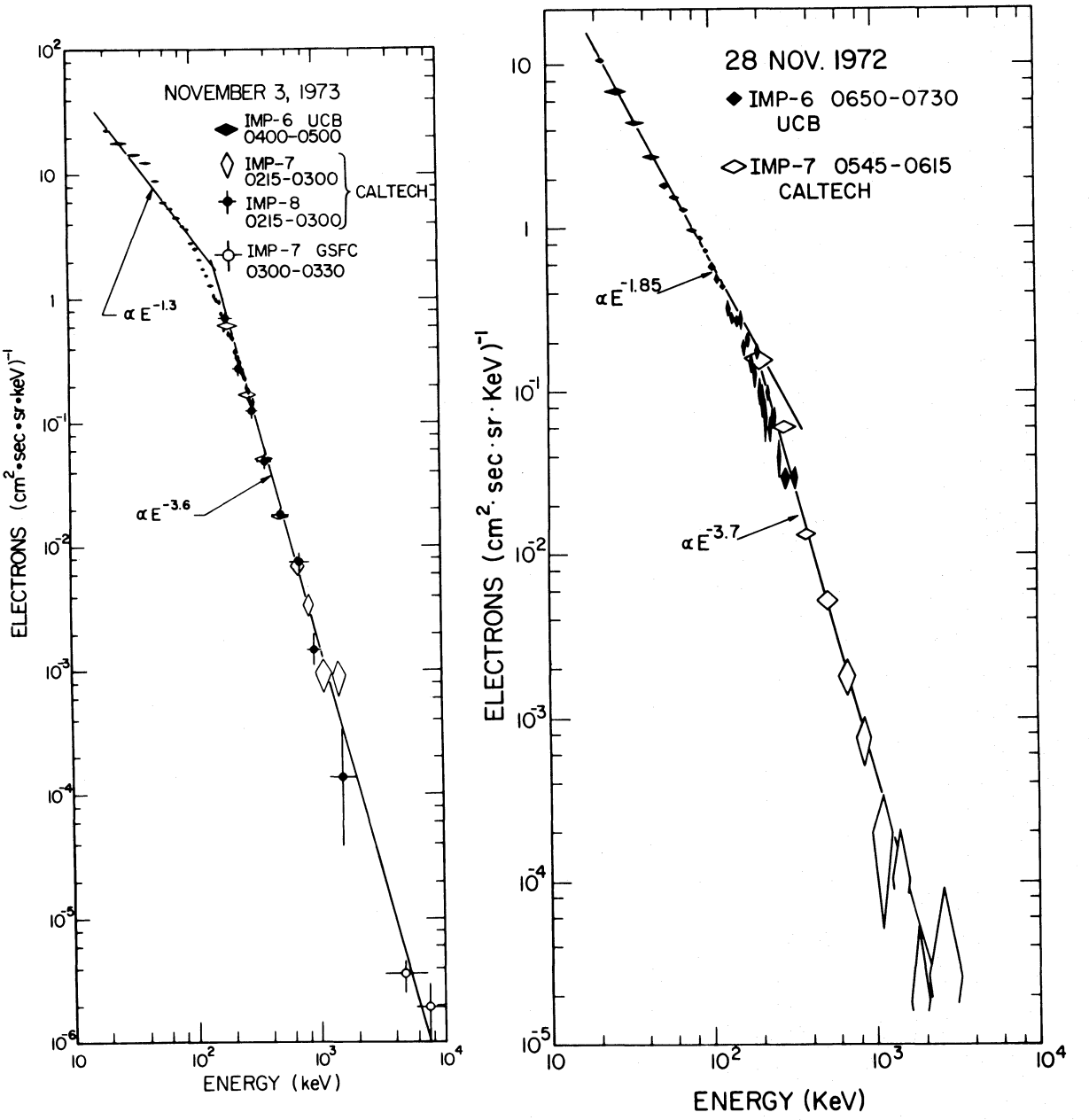

FIG. 6.—High resolution energy spectra for two more events. The 1973 November 3 event has some terrestrial particle contamination below ~50 keV. Above the ~200 keV there is close agreement between the *IMP 7* and *IMP 8* measurements. No steepening is observed above ~3 MeV for this event. The 1972 November 28 event does not have a measurable flux at energies above ~4 MeV.

the event maximum near 1000 UT. Figure 5*a* shows the energy spectrum. Here high resolution PHA data is available from the UCB experiment. Note the agreement in the region of overlapping measurements. Again a flat power law spectrum is observed below ~100 keV, changing to a much steeper power law at higher energies which extends to the limits of the measurements at ~3 MeV. Figure 5*b* shows the spectrum for the large event of 1973 April 30 where the spectrum extends to ~20 MeV. In this case, the GSFC data at ≥10 MeV are a factor of more than 5 below an extrapolation of the 0.2 to 2.0 MeV spectrum, providing clear evidence for a steepening of the spectrum at high energies.

Figure 6 shows two more events with PHA data from the UCB experiment. In the 1973 November 3 event, there was contamination at energies below ~100 keV from terrestrial particle fluxes before 0400, when the event maxima at those energies may have occurred.

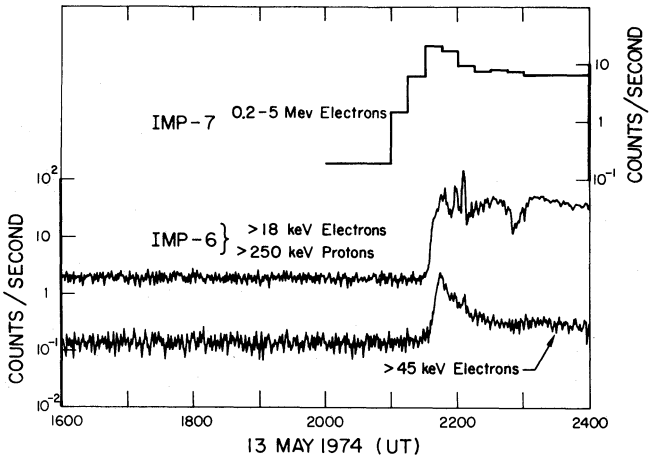

FIG. 7.—The 1974 May 13 scatter-free event

Even in the 0400–0500 period used for the spectral measurements, some terrestrial particles are present, probably accounting for the feature at ~50 keV. The spectrum in this event extends to ~10 MeV without apparent steepening at high energies.

Figure 7 shows the 1972 May 13 event which had a scatter-free profile (Lin 1970) at both low (≤100 keV) and high energies. The spectrum for this event is shown in Figure 8 along with those of three normal diffusive events.

All these energetic electron events thus have the same characteristic spectral shape. The main features are:

1. A power law spectrum $dJ/dE \propto E^{-\gamma}$ from below ~100 keV down to ~20 keV, the lower limit of the measurements. The index γ ranges from 0.6 to 2.0 (see Fig. 9).

2. A steeper power law, γ of 2.4 to 4.3 (Fig. 9) fits from above ~200 keV to typically ~2 MeV. Where counting statistics permit, this spectrum is observed up to ~20 MeV energy, although sometimes with a steepening at high energies.

3. A smooth transition is observed in the range ~100 keV to ~200 keV. If we define the "break" energy as the intersection of the extrapolation of the two power laws, this break occurs at ~140±40 keV, except for the 1974 May 13 scatter-free event where the break occurred at the anomalous low value of 80 keV. The break energy appears to be independent of flux and/or spectral hardness. The difference in the spectral indices for a given event is ~2 with a range from 1.7 to 3 (see Table 1). The lowest two values of γ (<100 keV) correspond to the lowest two values of γ (>200 keV) (Fig. 10).

4. The power law spectra, particularly below 100 keV, are observed to be harder for events with higher electron flux at 100 keV (Fig. 11).

5. There is no obvious dependence of any of the electron spectral parameters on solar longitude in the W30°–W90° longitude range (Figs. 12 and 13).

We have investigated a wide range of spectral forms (flux or density versus rigidity, velocity or energy, and also distribution functions, etc.), but none of them provides a simpler description of these electron spectra than the form used here. We note from equation (5) that the density rather than flux is related to the number, N, of escaping particles. The number spectrum dN/dE also fits to a double power law, but with larger power law exponents: below 100 keV typically the γ is 0.4 larger (steeper) and, between 0.2 and 2 MeV, about 0.2 larger. Above 2 MeV the slopes are unchanged.

V. DISCUSSION

We have compared our spectral measurements with those reported previously. At nonrelativistic energies only integral (>20 and >45 keV) channel data have been systematically studied before (Lin 1974). These show that the energy spectra for electron events in general are consistent with power law indices of ~3–4, but events associated with energetic protons and relativistic electrons (large flares) have substantially harder nonrelativistic spectra, consistent with our findings here of indices ranging from 0.6 to 2 below 100 keV. Previous observations of relativistic electrons with moderate energy resolution above ~3 MeV show that the spectrum is fit by a power law with index ~3–4 (Cline and McDonald 1968; Datlowe 1971), consistent with the results reported here. When the >3 MeV spectra were compared with 0.3–0.9 MeV broadband flux, occasional flattening was inferred between 3 MeV and ~1 MeV (see Simnett 1974 for review).

The solar events studied here have been included in a study of >0.2 MeV solar flare electrons by Decker and Armstrong (1979). They determined approximate values for the spectral index γ of 0.2 to 0.8 MeV electrons by comparing the counting rate in two energy intervals with the calculated response of their instrument. From

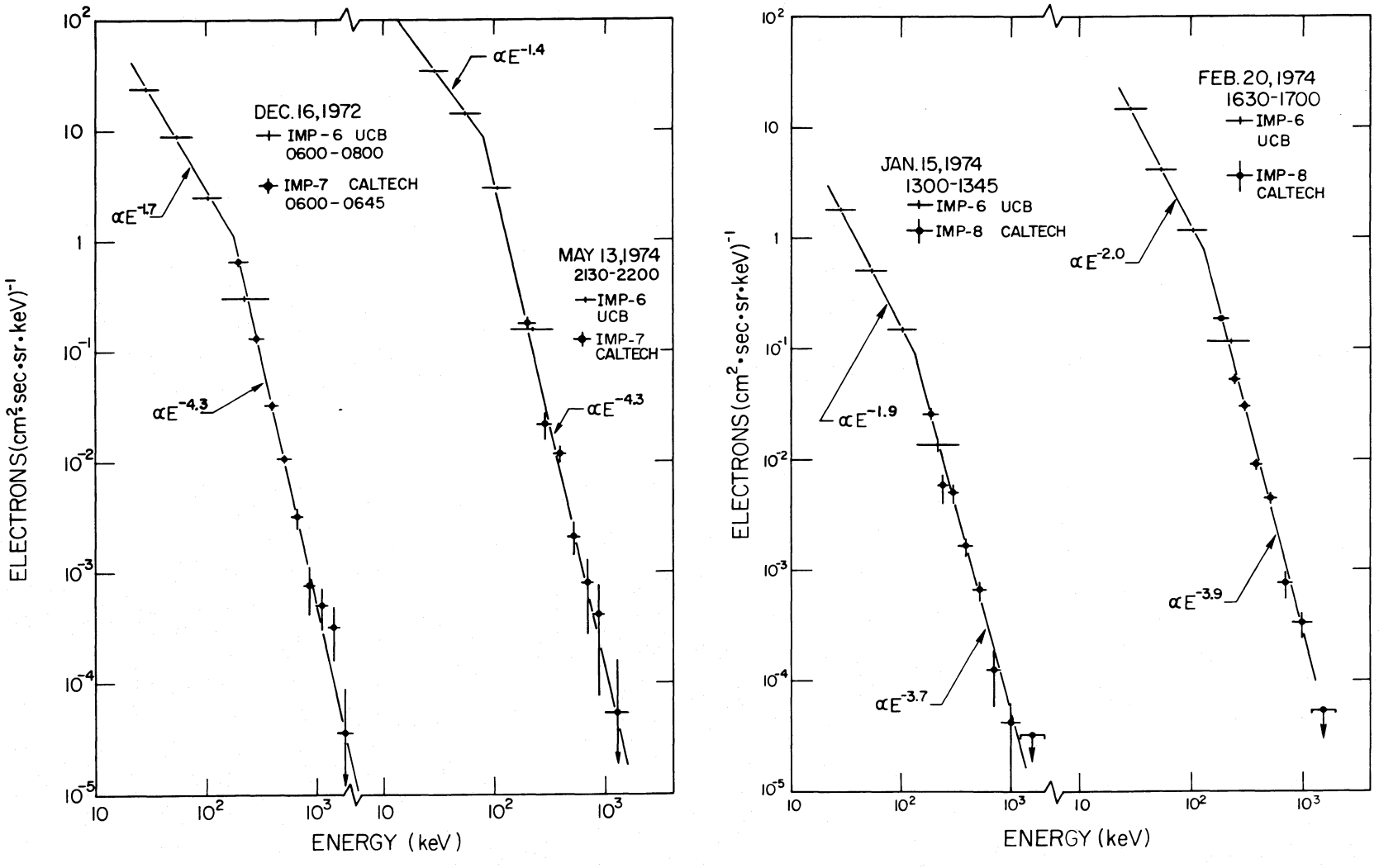

FIG. 8.—Spectra for four more events, including the 1974 May 13 scatter-free event. There are no high resolution UCB data for these events, but the May event appears to have an anomalously low break energy.

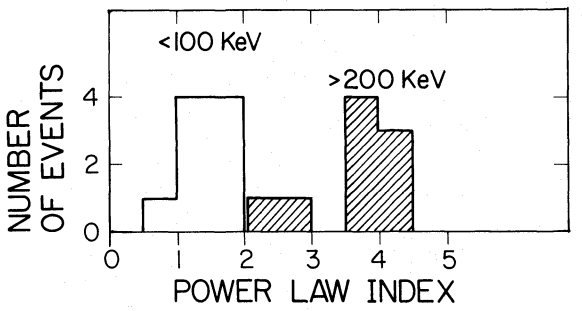

FIG. 9.—The number distribution of power law indices below 100 keV and above 200 keV.

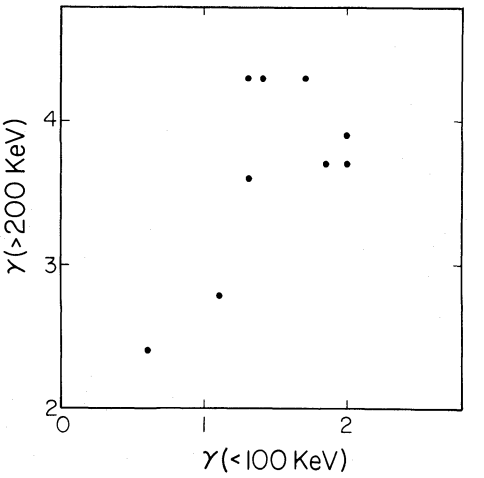

FIG. 10.—Plotted here is the spectral exponent below 100 keV vs. the exponent above 200 keV.

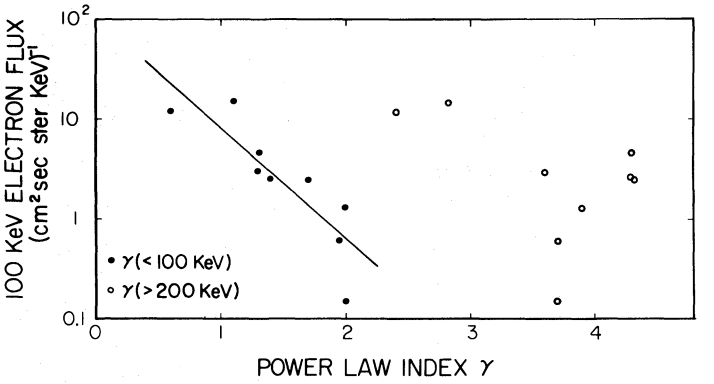

FIG. 11.—The spectral exponents are plotted here as a function of the 100 keV electron flux. There is a good correlation of the exponent below 100 keV with flux (*solid dots*) and a poorer correlation for the exponent above 200 keV (*open circles*).

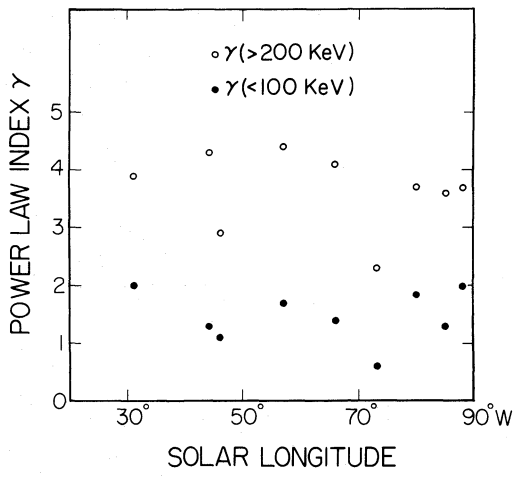

FIG. 12.—The distribution of power law indices below 100 keV (*solid dots*) and above 200 keV (*open circles*) as a function of solar longitude.

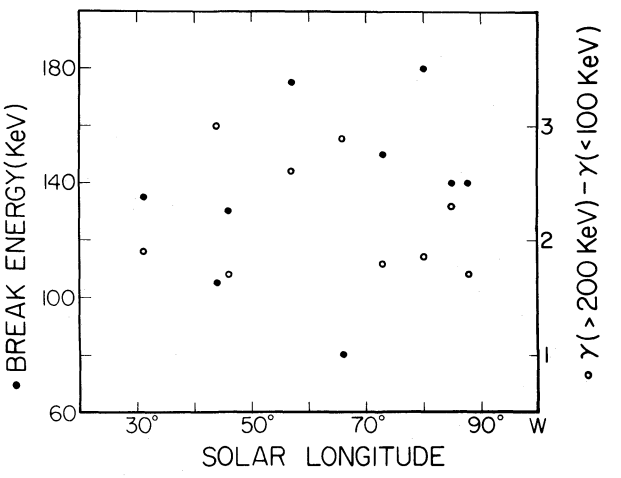

FIG. 13.—The distribution of break energy (*solid dots*) and difference in power law exponents (*open circles*) as a function of solar longitude of the flare.

a comparison of 15 solar events, we find a very good correlation of the spectral index measured by the Caltech experiments with that reported by Decker and Armstrong. The Caltech spectra are always softer, however, such that typically, $\Delta\gamma = 1.0 \pm 0.2$. According to Decker and Armstrong, this systematic difference may arise because the actual electron response of their detector differs from the ideal response assumed in their calculation.

The most characteristic spectral feature we observe is the break near 100 keV. We have considered several possible origins for this feature. Although the break is always contained entirely within the *IMP 6* UCB experiment energy range, there is no indication that it is due to instrumental effects. The spectrum at low energies is consistent with previous Geiger-Müller detector measurements (Lin 1974), and the break is also observed in large solar events with an entirely different configuration of semiconductor detector telescopes on the *ISEE-3* spacecraft (experiment description in Anderson *et al.* 1978).

The observed break is unlikely to be due to interplanetary propagation. We have shown that the spectra constructed in the above manner correspond to the spectra of the electrons injected at the Sun. The interplanetary propagation characteristics of these electrons show little variation over the entire energy range and certainly no sudden change around 100–200 keV.

We have also considered the possibility that the initial accelerated electron spectrum is a single power law extending over the entire energy range, and that Coulomb energy loss of these electrons passing through the solar atmosphere then produces the break. To produce the typical flattening observed at ~ 100 keV requires passage of the electrons through a column density of ionized hydrogen of $\sim 10^{21}$ cm^{-2}. Passage through this much matter would, however, produce a turnover in the electron spectrum at ~ 40–50 keV (see Lin 1974). This is not observed.

The observed escaping electron spectra reported here are also generally consistent with the hard X-ray and microwave spectra typically observed from large flares. Hard X-ray bursts for large flares have systematically much harder spectra, X-ray power law indices of $\gamma_x < 2$–3 below 100 keV, than typical small flares ($\gamma_x \gtrsim 4$). For the 1972 August 4 large flare a break to a steeper power law spectrum above ~ 100 keV energies was observed in the hard X-ray spectrum (Hoyng 1975). This X-ray break implies a break in the bremsstrahlung producing electrons at ~ 140 keV (Ramaty, Kozlovsky, and Lingenfelter 1975). A similar break at ~ 100 keV is reported in the X-ray spectrum for an over the limb flare event on 1972 July 22 (Hudson, Lin, and Stewart 1981), and during the impulsive phase of the 1969 March 30 large flare (Frost and Dennis 1971). The reported X-ray power law indices are typically $\gamma_x \sim 2$ below and $\gamma_x \sim 4$ above the break. These correspond to electron indices of ~ 1.5 and ~ 3.5, respectively, consistent with the results reported here. It is unlikely, then, that the break in the spectrum of the escaping electrons is due to preferential trapping of the <100 keV electrons at the Sun.

Microwave spectra at high frequencies, where absorption should be negligible, suggest typical spectral indices of ~ 3 for several MeV energy electrons (Ramaty and Petrosian 1972), consistent with those reported here. We find (Fig. 14) a good correlation of the maximum microwave ($\lambda = 10$ cm) burst intensity and escaping >20 keV electron fluxes. The 10 cm microwave flux has been shown to be quantitatively correlated to the >20 keV hard X-ray emission (Kane 1972). From the inferred hard X-ray emission, we can obtain a lower limit to the number of electrons at the Sun (see Lin 1974). This gives $\gtrsim 10^{36}$–10^{38} electrons above 20 keV compared to $\sim 10^{33}$–10^{35} escaping (eq. [7]). Thus, as found before (Lin and Hudson 1976), only ~ 0.1–1% of the accelerated electrons escape. The correlation of Figure 14 implies that the electron escape efficiency does not vary by more than about one order of magnitude from event to event. The good microwave-electron correlation and the lack of any longitude dependence indicate that escape and propagation effects are not significant for flares located in the W30°–W90° longitude range. In this respect the electrons are similar to the 20–80 MeV protons studied by Van Hollebeke, MaSung, and McDonald (1975).

The general agreement of electron spectra with hard X-ray and microwave spectra suggests that the escaping electrons are a representative sampling of the electron population at the Sun and that the break in the spectra at 100–200 keV is not due to a rigidity or energy

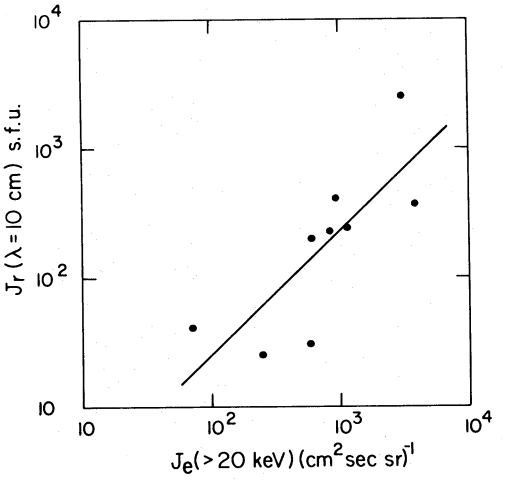

FIG. 14.—Shown here is the correlation between the maximum microwave radio flux at 10 cm wavelength and the >20 keV electron flux.

dependent escape process. However, further studies, utilizing detailed comparisons of good quality X-ray and radio spectra with escaping electron spectra for the same flares, are needed.

We have also investigated whether the ions which are accelerated in the large flares have a similar characteristic spectrum and whether that spectrum is related to that of the electrons. Van Hollebeke, MaSung, and McDonald (1975) found that proton spectra in the ~10–80 MeV range generally fit well to a power law. We have plotted in Figure 15 the best fit proton power law spectral index in the >10 MeV energy range, as measured by the GSFC instruments, versus the <0.1 MeV electron spectral index for eight of the events studied here. As can be seen, the electron and proton spectra appear correlated. Comparisons with the >0.2 MeV electron spectral indices, however, yield little if any correlation. It may be significant that 10–80 MeV protons have approximately the same velocities as 5–40 keV electrons.

The spectral correlation in Figure 15 suggests that the electrons and protons are accelerated by the same mechanism. For velocity dependent acceleration, the break in the electron spectra at 100–200 keV would imply a similar break at ~200–400 MeV for protons. Although a characteristic sharp break has not been reported for protons at these energies, steepening of the spectra at a few hundred MeV is often observed (Fichtel and McDonald 1967). On the other hand, proton spectra are commonly observed with a bend or break near 1–10 MeV (Van Hollebeke 1978). At energies below 10 MeV, however, the proton spectra may be strongly affected by convection/energy change processes in the propagation of these relatively slow particles from the Sun to 1 AU.

The results reported here support the general picture of two distinct types of particle accelerating flares: those which effectively accelerate only electrons with energies below ~100 keV, and those large flares which also accelerate electrons up to relativistic energies and protons as well. We find here that events with relativistic (>200 keV) electrons are always accompanied by proton acceleration, type II and IV radio emission, etc. Based on the timing sequences observed in hard X-ray (Frost and Dennis 1971), gamma-ray (Bai and Ramaty 1976), radio (Wild, Smerd, and Weiss 1963), and energetic particle (Lin 1974) phenomena associated with the large flare events, it appears that following the impulsive <100 keV electron acceleration a second phase of acceleration occurs which is closely associated with the passage of a flare shock wave through the corona. Interplanetary propagation effectively merges the particle contributions from the first and second phase acceleration by the time of the particle event maximum at 1 AU. What we observe, therefore, is a combination of the two acceleration processes. The fact that a single characteristic shape is observed for every event with very

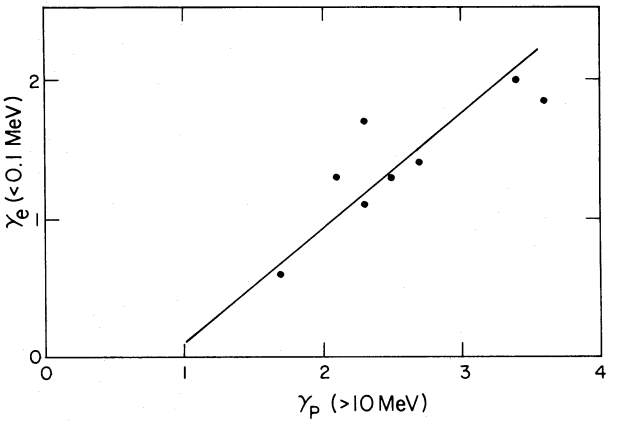

FIG. 15.—Plotted here is the electron spectral exponent below 100 keV vs. the proton spectral exponent above 10 MeV, obtained from the GSFC instruments on *IMP 7* and *IMP 8*. One event is missing because the proton flux above 10 MeV is too low to define the spectrum.

little variation in break energy suggests, however, that a single acceleration phase dominates; or that the lower energy $\lesssim$100 keV component is closely related to the >200 keV component, perhaps as an injection source for the acceleration of the high energy component (cf. Ramaty *et al.* 1980).

The flare shock wave at the Sun is visible through the type II radio burst emission it produces, and often it is also observed a day or two later near the Earth as an interplanetary shock. Both theoretical (Ramaty *et al.* 1980) and observational evidence (Gloeckler *et al.* 1976; Hudson, Lin, and Stewart 1981) suggest that this shock wave is the accelerating agent for the electrons and ions observed in these large flare events. The results reported here indicate that the shock accelerates particles by a velocity-dependent mechanism. Particle acceleration at shocks by a drift ($\bar{v}_{\rm shock} \times \bar{B}$) mechanism and/or by Fermi process in the preshock and postshock turbulence would give a dependence on velocity (Armstrong *et al.* 1977; Pesses, Decker, and Armstrong 1981; Ramaty *et al.* 1980).

VI. CONCLUSIONS

We have shown that the electron spectra from large flare events have a characteristic double power law shape over the energy range 20 keV to several MeV. On the occasions when the fluxes are high enough, this spectrum is seen to extend to >20 MeV, although some steepening is sometimes observed at the highest energies. Based on the propagation analysis and on the similarity of these electron energy spectra to those inferred from hard X-ray and microwave emission, we believe that we are in fact sampling the spectrum of electrons accelerated at the Sun. The good correlation of electron flux to microwave intensity indicates that the electron escape

efficiency does not vary by more than an order of magnitude from event to event. We find that the stronger the acceleration, the harder the electron spectrum produced. Furthermore, the accelerated proton spectrum for these events appears correlated to the spectrum of electrons with approximately the same velocity. We wish to note here, however, that these conclusions are based on events observed on the descending phase of the solar cycle, well past maximum.

We believe that these particles are accelerated by the flare shock wave as it passes through the solar corona. The spectra observed here may be characteristic of the collisionless shock acceleration process. We note that flare shock waves in the interplanetary medium near 1 AU, corotating shock waves in the distant heliosphere, and bow shocks in front of planetary magnetospheres all accelerate particles to similar spectral shapes (Lin 1980), although the energy ranges and flux levels are vastly different. This may, therefore, be a canonical shape for particles accelerated by collisionless shock waves.

We wish to thank F. B. McDonald and R. E. McGuire for providing information on the GSFC detector system. Berndt Iwers provided valuable assistance with the GSFC data analysis. One of us (R. A. M.) wishes to thank E. C. Stone for many fruitful discussions. The research at the University of California was supported in part by NASA grant NGL-05-003-017. The work at Caltech was supported in part by NASA under contract NAS 5-11066 and NAS 5-25789 and grant NGR-05-002-160.

REFERENCES

Anderson, K. A., Lin, R. P., Potter, D. W. and Heetderks, H. D. 1977, *IEEE Trans.*, **GE-16**, 153.
Armstrong, T. P., Chen, G., Sarris, E. T., and Krimigis, S. M. 1977, in *Study of Travelling Interplanetary Phenomena*, ed. M. A. Shea *et al.* (Dordrecht: Reidel), p. 367.
Bai, T., and Ramaty, R. 1976, *Solar Phys.*, **49**, 343.
Baker, D. N., and Stone, E. C. 1977, *J. Geophys. Res.*, **82**, 1532.
Cline, T. L., and McDonald, F. B. 1968, *Solar Phys.*, **5**, 507.
Datlowe, D. 1971, *Solar Phys.*, **17**, 436.
Decker, R. B., and Armstrong, T. P. 1979, *J. Geophys. Res.*, **84**, 7334.
Fichtel, C. E., and McDonald, F. B. 1967, *Ann. Rev. Astr. Ap.*, **5**, 351.
Frost, K. J., and Dennis, B. R. 1971, *Ap. J.*, **165**, 655.
Gloeckler, G., Sciambi, R. K., Fan, C. Y., and Hovestadt, D. 1976, *Ap. J. (Letters)*, **209**, L93.
Hamilton, D. C. 1977, *J. Geophys. Res.*, **82**, 2157.
Hoyng, P. 1975, Ph.D. thesis, University of Utrecht, The Netherlands.
Hudson, H. S., Lin, R. P., and Stewart, R. T. 1981, *Solar Phys.*, in press.
Hurford, G. J., Mewaldt, R. A., Stone, E. C., and Vogt, R. E. 1974, *Ap. J.*, **192**, 541.
Kane, S. R. 1972, *Solar Phys.*, **27**, 174.
Krimigis, S. M. 1965, *J. Geophys. Res.*, **70**, 2943.
Lin, R. P. 1970, *J. Geophys. Res.*, **75**, 2583.
_____. 1971, *Solar Phys.*, **12**, 209.
_____. 1974, *Space Sci. Rev.*, **16**, 189.
Lin, R. P. 1980, *Solar Phys.*, **67**, 393.
Lin, R. P., Meng, C. I., and Anderson, K. A. 1974, *J. Geophys. Res.*, **79**, 489.
Lin, R. P., and Hudson, H. S. 1976, *Solar Phys.*, **50**, 153.
Mewaldt, R. A., Stone, E. C., and Vogt, R. E. 1977, *Space Sci. Instr.*, **3**, 231.
Parker, E. N. 1963, *Interplanetary Dynamical Processes* (New York: Wiley-Interscience), Chap. 8.
Pesses, M., Decker, R. B., and Armstrong, T. P. 1981, *Space Sci. Rev.*, in press.
Potter, D. W., Lin, R. P., and Anderson, K. A. 1980, *Ap. J. (Letters)*, **236**, L97.
Ramaty, R., Kozlovsky, B., and Lingenfelter, R. E. 1975, *Space Sci. Rev.*, **18**, 341.
Ramaty, R., Kozlovsky, B., and Suri, A. N. 1977, *Ap. J.*, **214**, 617.
Ramaty, R., *et al.* 1980, in *Solar Flares*, ed. P. A. Sturrock (Boulder: Colorado Associated University Press), Chap. 4, p. 117.
Ramaty, R., and Petrosian, V. 1972, *Ap. J.*, **178**, 241.
Simnett, G. M. 1974, *Space Sci. Rev.*, **16**, 257.
Simnett, G. M., and McDonald, F. B. 1969, *Ap. J.*, **157**, 1435.
Van Hollebeke, M. A. I. 1978, in *A Close-Up of The Sun*, ed. M. Neugebauer and R. W. Davies, JPL Pub. 78-70, p. 205.
Van Hollebeke, M. A. I., MaSung, L. S., and McDonald, F. B. 1975, *Solar Phys.*, **41**, 189.
Wild, J. P., Smerd, S. F., and Weiss, A. A. 1963, *Ann. Rev. Astr. Ap.*, **1**, 291.

R. P. LIN: Space Sciences Laboratory, University of California, Berkeley, CA 94720

R. A. MEWALDT: 220-47 Downs Laboratory, California Institute of Technology, Pasadena, CA 91125

M. A. I. VAN HOLLEBEKE: Code 661, NASA/Goddard Space Flight Center, Greenbelt, MD 20771